EXPLOITATION OF SOME MICRO-MECHANICAL CONCEPTS TO DEVELOP AN ENGINEERING MODEL OF SHOCK INITIATION

Philip M. Howe
Los Alamos National Laboratory
P.O. Box 1663
Los Alamos, New Mexico, 87544

and

David C. Benson
University of California, San Diego
Department of Mechanical and Aeronautical Engineering
9500 Gilman Drive
La Jolla, California 92037-0411

We have used a two-dimensional Eulerian hydrocode to explore the utility of various micro-mechanical concepts for the development of an engineering model for shock initiation of plastic bonded explosives. Our goal was to develop a shock initiation model that would accurately describe the existing shock initiation data in terms of physically measurable or calculable quantities. We used a simple Arrhenius fit to experimental data to describe the decomposition of the explosive (PBX 9501) in hotspots and in the bulk explosive. We ignored any contribution from the binder reactions to the chemical kinetics. Experimentally measured micrographs of PBX 9501 were used to develop microstructures for use in the hydrocode. In the code, such structures were subjected to shock inputs of various strengths, and temperature distributions in binder, pure HMX, and hotspots were calculated. This allowed us to relate the various temperature distributions to the bulk temperature and calculate various reaction rates. A simplistic erosive burning mechanism was used in competition to bulk burning to describe the post-ignition reaction spread. The energy release rate resulting from the competition of these reactions was used as input to a method of characteristics code. This in turn was used to calculate particle velocity – time profiles at various simulated gauge locations. These calculated profiles were compared with experiment.

INTRODUCTION

There is a very rich literature on shock initiation[1]. Two sets of papers that we found particularly useful in guiding our thinking were those of Kim[2] and Partom[3]. In addition, a variety of micromechanical concepts has been used to guide model development. Thus, hotspot concepts have been advanced that involve cavity collapse, intergranular friction, plastic work, viscous heating, inter alia. In some instances it has been assumed that the hotspots form, react, add their energy to the system and extinguish. In others, a critical condition is applied for the hotspot to grow, and a nucleation and growth mechanism is used. Typical assumptions for the growth mechanisms

involve concepts such as grain burning or hole burning, or combinations of the two. In implementation, an average hotspot size and temperature are usually assumed. The collection of assumptions usually forces the model away from measurable input parameters.

In this effort, we used the calculated shock response of two dimensional microstructures to help develop the framework of an initiation model. We also used it to describe the temperature distribution for hotspots generated at grain boundaries and surrounding voids, related these temperature distributions to bulk temperatures, and those in turn to state variables at the shock front. We used an experimentally determined rate equation for PBX 9501 decomposition, and an experimentally determined Hugoniot. We also used an experimentally determined function to describe the linear erosion rate and its dependence upon pressure, although this was extrapolated well beyond the regime where there is data. In addition, we had to create a topology function for erosive burning that was without any theoretical or experimental support, and had to treat the representative hotspot temperatures as fitting parameters, although the functional dependence upon shock strength was guided by the microstructure calculations.

MICROSTRUCTURES AND CALCULATED TEMPERATURE DISTRIBUTIONS

Skidmore et al have characterized the microstructure of PBX 9501[4]. PBX 9501 is an HMX-based plastic bonded explosive with 95% by weight HMX and 5 % by weight binder. The binder is a mixture of a polyurethane and a nitroplasticizer. The HMX moiety is composed of a large and small particle size distribution. The material is formed into prills, and hot-pressed to a density in the range 1.834 – 1.838 g/cm^3. Representative microstructures are shown in Skidmore[4]. It turns out that a significant fraction of the small particle size HMX is either dissolved in the binder or is below the resolution of the microscopy. We therefore modeled the binder as a viscoelastic material representative of pure binder, but with the energetics of a mixture of binder, nitroplasticizer, and HMX. An algorithm developed by Benson was used to translate the micrographs into descriptions that could be treated in the hydrocode[5]. Representative computer generated micrographs are shown in Conley[6].

The computational microstructures were subjected to step shocks of varying strengths. A description of the nature of the calculations is given in Conley[6]. Distributions in binder temperature, HMX temperature, and bulk temperature were calculated as a function of shock strength. HMX, binder, and void induced hotspot temperature distributions were correlated with calculated bulk temperatures. This allowed us the option to consider different equations of state for the unreacted material bulk temperature. This implies the assumption that the interrelationship between the various temperature distributions is independent of the nature of the equation of state for the bulk unreacted material, which is not likely to be generally true.

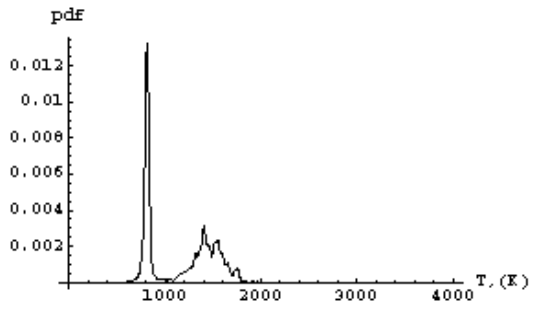

FIGURE 1: DISTRIBUTION FUNCTIONS FOR THE HMX AND INTERGRANULAR HOTSPOT TEMPERATURES

A calculated temperature distribution for binder and HMX are shown in Figure 1.The input shock had a particle velocity of 1500m/s, The two temperature distributions are not to scale. Since the HMX-enriched binder and HMX crystals were treated as separate materials, it was easy to calculate separate temperature distributions for each. When we used these distributions to calculate ignition at various shock strengths, we found that the temperatures distributions led to too little reaction to provide physically meaningful ignition thresholds. We therefore performed additional calculations to determine temperature distributions for void induced hotspots. These distributions were more difficult to describe, as the material that is heated is the surrounding HMX or HMX/binder, depending upon hotspot location. The proper approach to calculate the energy released from ignition reactions would be to integrate the reaction rate over the temperature distribution. This was computationally inefficient, and we used the variation of peak temperatures with particle velocity to ascribe reference temperatures for calculations. We were able to express the peak hotspot temperatures as linear functions of the bulk temperature. We then calculated the bulk temperature, using Davis' equation of state, as a function of shock strength[7].

HOTSPOT FORMATION AND EROSIVE BURNING

Upon examination of the temperature spatial distribution in representative shocked microstructures, it became immediately apparent that it would not be easy to relate hotspot size and shape distributions to microstructure morphology, and that the dependence of the erosive burning upon microstructure was likely to be complicated. The treatment of choice would involve modeling the microstructures in 3-D, with inclusion of appropriate transport processes to allow us to generate an erosive burning function that captured the correct morphological dependence. This could be then correlated with experimentally determined burn rates. The inefficiencies associated with fully 3-D calculations caused us to take a less ambitious approach. Thus, for the calculations presented here, we extracted temperature distributions from the shocked synthetic microstructures, and used them to calculate energy release rates and times associated with ignition processes. We then introduced a purely empirical function to describe the erosive burning.

Since we elected not to conduct three dimensional erosive burning calculations to generate a surface regression function, we have little knowledge of what the actual function should be, except that the extent of reaction must start off at some function determined by the hotspot size and temperature distributions, must go through a maximum, and return to zero

at completion of reaction. We thus chose the logistic function as a reasonable form with which to start. When fitting the data, we found that a modification to the logistic form was necessary (see below).

There are numerous instances in the literature where linear burn rates are described by an expression of the sort $g(t)= a P^n$, where n is a value near unity. However, the range over which such correlations are available do not extend into the regime of interest. Nonetheless, we used this expression to describe the dependence of the linear burn rate upon shock strength.

We have no theoretical reason for expecting the linear burn rate to be a function of state variables at the shock front rather than the pressure or particle velocity in the following flow. This is an assumption that is made, that may have to be adjusted in the future.

EQUATION OF STATE FOR THE UNREACTED AND REACTED MATERIAL

Experimental values for the Hugoniot in the shock velocity – particle velocity plane were taken from Gustavsen[8]. Davis' equation of state was calibrated by making the assumption that the bulk temperature for the unreacted solid at the von Neuman spike was such that the reaction zone thickness for a steady detonation would correspond to the value estimated by Sheffield[9] from experiment. In this sense, the equation of state for the unreacted material is tied to the chemical kinetics. It also implicitly includes the assumption that bulk burning is important at the detonation point. In our calculations, we found that erosive burning dominated over most of the shock initiation domain, but that bulk burning could dominate near and at the detonation state. The competition between these two processes influences the shape of the particle velocity wave profiles.

A method of characteristics code was calibrated to the Hugoniot for PBX 9501 and a final state that matched the experimental detonation velocity. Davis' equation of state for the unreacted material was used to calculate an unreacted bulk temperature behind the shock as a function of shock particle velocity. Temperatures for the hotspots formed from voids in crystals and at crystal interfaces were related to the bulk temperature. The actual values of hotspot temperatures at a given shock strength are expected to be a function of the nature of the shock heating mechanisms. The hydrocode we used contained cold compression, which contributed only a very small effect, viscous heating, frictional heating between grains, and plastic work. An explicit description of shear band formation was not included.

We assigned a representative temperature to the hotspot distributions for each of the two types of hotspots, (using the maximum values for the distributions) and used that single temperature to calculate reaction rates, rather than integrate the reaction rates over the temperature distribution. This introduces an additional degree of empiricism, but greatly increased the speed of the calculations.

A progress variable (the extent of reaction) whose rate was tied to the bulk and hotspot temperatures calculated using Davis' equation of state was used

to describe the energy release rate and transition from unreacted material to products. The product equation of state has no direct influence upon the rates of reaction since, in this model, they are all tied to variables at the shock front.

CHEMICAL KINETICS

Henson et al[10] have developed a model set of chemical kinetics that they have applied to PBX 9501 subjected to various thermal environments. Their model consists of a set of reactions that can be collected into a set of three aggregate steps. The first step is an endothermic solid – solid phase transition, whose rate is described by a nucleation and growth mechanism. The second step is a solid – gas set of reactions that can be weakly endothermic or exothermic, depending upon conditions. The third step is a strongly exothermic set of reactions, that provides the major energy release. Under conditions of interest, the first two steps are slow, and rate determining.

Henson et al have shown that the kinetics can be applied over many decades of temperature. They have also shown that the kinetics model can be collapsed into a single Arrhenius equation, with some loss of accuracy. We used the single Arrhenius equation as a rate law to describe hotspot reactions and bulk reactions. We have also made the assumption that the rates can be tied to a temperature associated with the unreacted solid. The temperature of the solid material is strongly dependent upon shock strength (through Davis' equation of state) but only weakly dependent upon the pressure behind the shock. This is because the pressure provides only a small contribution to the solid heating. This allows us to relate the rate laws to the hotspot and bulk temperatures at the shock front.

THE EQUATION SET

Using Davis' equation of state, the bulk temperature can be expressed in terms of the particle velocity at the shock front by the equation

$$T_b = T_0 \left\{ 1 + \frac{u_p^2}{2} \frac{(1+a)}{c_{v0}\, T_0} \right\}^{\frac{1}{1+a}}$$

where

T_b is the bulk temperature,
T_0 = 298 K,
u_p is the particle velocity at the shock front,
α = 1.008 a constant (value chosen in range reported by Davis[7]).
c_{v0} = 1088 J/kg/K is the constant volume heat capacity.

The bulk temperature is the mass weighted temperature for void collapse induced hotspots, hotspot material formed at grain boundaries, and the HMX material that is heated only by shock compression. The equation for the temperature of hotspots formed at grain boundaries is given by

$$T_1 = T_0 + c_1 (T_b - T_0)$$

where
T_1 is the hotspot temperature and
c_1 = 2.4 is a fitting constant.

Similarly, the equation for the temperature of hotspots formed by void collapse is given by

$$T_3 = T_0 + c_3 (T_b - T_0)$$

where $c_3 = 6.5$ is a fitting constant.

The temperature for the HMX that is heated only by shock compression is then

$$T_2 = \frac{T_b - m_1 T_1 - m_2 T_3}{1 - m_1 - m_2}$$

where
m_1 is the mass fraction of material forming hotspots formed at grain boundaries,
m_2 is the mass fraction of hotspot material formed by void collapse.

Both m_1 and m_2 are treated as fitting parameters although, in principle, their values could be extracted from the hydrocode calculations. For our early calculations, we treated both m_1 and m_2 as independent of u_p. However, the hotspot masses clearly increase in size with increasing shock strength. In our later calculations, we gave them a linear dependence upon particle velocity at the shock front. Calculated temperatures as functions of particle velocity at the shock front are shown in Figure 2. Slopes of curves increase in order T_2, T_b, T_1, T_3.

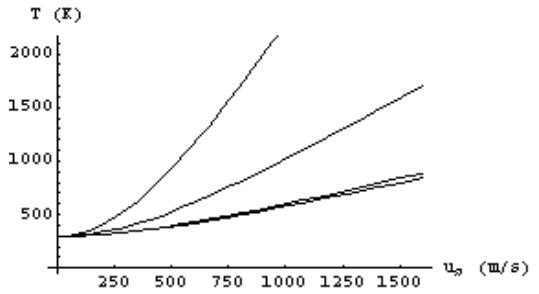

FIGURE2: TEMPERATURES VS PARTICLE VELOCITY AT THE SHOCK FRONT

The chemical kinetics were treated by a single Arrhenius rate, using values provided by Henson, and incorporating the heat of reaction and applying an adiabatic condition. The chemical rate equation used to describe the rate of evolution of both types of hotspots and bulk reaction is

$$y_x'(t) = k_0 (1 - y_x(t)) \; e^{-\frac{E_{act}}{R\,T_x + \frac{y_x(t)\,q}{c_{v0}}}}$$

where
x is 1, 2, or 3, for the ignition reaction induced by hotspot formation at grain boundaries, reaction in bulk, or by ignition induced by void collapse,
R is the natural gas constant,
q = 6650 J/g is the heat of reaction,
$Eact$ = 149000 J/mol is the energy of activation, and
k_0 = 5.578 x 10^6 prefactor

We described erosive burning by a product of a topology function intended to capture the geometrical effects of the spread of the erosive burn front and an empirical aP^n description of the pressure dependence of the linear burn rate. Thus,

$$x'(t) = (x(t))^w \; (1 - x(t)) \; (sa_1 \, y_1(t) + sa_2 \, y_2(t)) \; (a \, u_p + s \, u_p)^n$$

where
a =1 x 10^{-7}, a value used to provide a linear burning rate of 100 m/s at a pressure of 100 Kbar,
w = 0.8, a fitting parameter, and
n = 1, the linear burning rate exponent.
$x'(t)$ is the rate of formation of product as a result of erosive burning,
sa_1 = 200 m_1 is the initial surface area for burning contributed by hotspots formed at grain boundaries,
sa_2 = 4700 m_2 is the initial surface area for burning contributed by hotspots formed from void collapse,

ρ_0 = 1.837, the bulk density of PBX 9501 used for comparison$c$ = 2.4 Km/s, s = 0.24. (The values for c and s were provided by Gustavsen for the PBX 9501 Hugoniot[11].)

The amount of product formed per unit volume at a given time is given by the sum of the material formed as a result of ignition in hotspots, the erosive burning, and bulk reaction. We expressed this as

$$c = c_b(t)\,(1-x(t)) + (c_{bg}(t) + c_e(t))\,x(t) + m_1\,y_1(t) + m_2\,y_2(t)$$

where
c_b(t) is the concentration of product formed by bulk reaction in the material unprocessed at a particular time by the erosive burn front,
c_{bg}(t) is the concentration of material formed by bulk reaction in the region processed by the erosive burn front,
c_e(t) is the concentration of material formed by erosive burning in the volume fraction processed by the erosive burn front, and $x(t)$ is the volume fraction of material processed by the erosive burning front at time t.

The balance equation, above, provides an overall rate of product formation

$$c'(t) = (1-x(t))\,c_b'(t) + x(t)\,(c_{bg}'(t) + c_g'(t)) - c_b(t)\,x'(t) + (c_{bg}(t) + c_g(t))\,x'(t) + m_1\,y_1'(t) + m_2\,y_2'(t)$$

This equation, times the heat of reaction, gives the energy release rate. This set of equations, together with initial conditions

$y_1(0) = y_2(0) = c_b(0) = c_g(0) = c_e(0) = x(0)$ and $x(0) = m_1 + m_2$.

solved simultaneously in Mathematica to provide a global volumetric energy release rate.

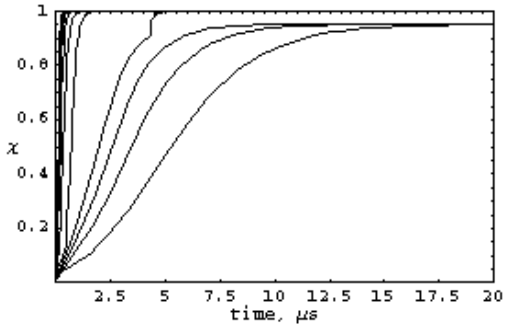

FIGURE 3: EXTENT OF REACTION AS A FUNCTION OF TIME FOR VARIOUS PARTICLE VELOCITIES

This energy release rate was used in a method of characteristics code to calculate particle velocity profiles at various simulated gauge locations. These in turn were compared with experimental data generated by Gustavsen et al. Plots of extent of reaction as a function of time for different particle velocities at the shock front are shown in Figure 3. The break in the curve is a result of igntions in hotspots at grain boundaries occurring and accelerating the erosive burning.

A FIT TO EXPERIMENTAL DATA

Gustavsen has reported experimental data on the shock initiation of PBX 9501. His results for an input shock particle velocity of 670 m/s and our calculated results are shown in Figure 4. The solid lines are data from Gustavsen and the dashed gray lines are calculated using this model. The general trend of the data shown in Figure 4 is captured rather well by the calculations. However, comparison with individual

gauge records shows that the shape of the curve behind the shock is not well represented over the entire range of data, although shock time of arrival and strength are well described.

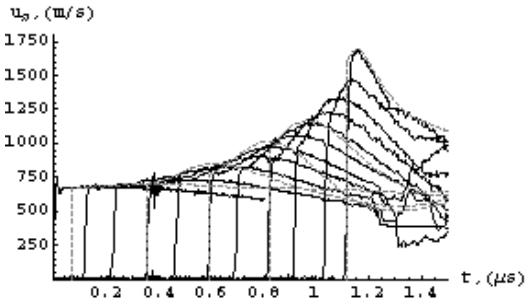

FIGURE 4: CALCULATED AND EXPERIMENTAL PARTICLE VELOCITY PROFILES.

DISCUSSION

In this model, the shock strength over the early part of the buildup process is almost entirely controlled by the ignition reactions. The hotspots formed as a result of void collapse are much more important at low shock strengths than are the hotspots generated at grain boundaries, which tend to be much cooler.

As the detonation state is approached, the relative contribution of the erosive burning mechanism increases. At the detonation state, bulk burning or erosive burning dominates, depending upon the choice of fitting parameters used in this model. The shock time of arrival at gauge points is controlled by the Hugoniot and the shock strength. The shock time of arrival is captured within the accuracy of the data. As the shock transitions to a detonation, the early following flow is captured with surprising fidelity.

The inclusion of two ignition mechanisms in our model to capture effects of hotspots formed at grain boundaries and by void collapse seems realistic. There is considerable physical evidence indicating that voids are especially efficient hotspot generators. Indeed, eliminating porosity from explosives has been a driver in explosives formulations for years. In this model, the kink in the curve of the following flow is caused by ignitions at grain boundaries causing additional energy to be released in the flow and an acceleration of erosive burning due to the additional ignited material.

The erosive burning model that we used is overly simplistic and does not properly capture the experimental behaviors. Three-dimensional calculations of the effects of particle morphology and size distribution upon erosive burning should be helpful.

SUMMARY AND CONCLUSIONS

Our goal was to use hydrocode modeling of realistic microstructures to examine various hypotheses regarding how initiation occurs. We wished to see if we could place them on a firmer physical basis and introduce them into engineering models in a way that would tie the parameters to physically measurable quantities. We were only partially successful. In the trade-off between model simplicity and use of physically meaningful input parameters, we erred on the side of simplicity and were forced to introduce some fitting parameters. We ended up with a set of seven fitting parameters, (c_1, c_2, m_1, m_2, sa_1, sa_2, w) which was far more than we liked. The first two are necessitated by

our choice to use representative temperatures rather than full temperature distributions to describe the hotspot temperature dependence upon particle velocity. (Recall that, since the hotspots generated by voids and intergranular boundaries in the microstructure had fairly broad distributions, we replaced the distributions by representative temperatures, whose dependence upon shock strength was calculated, but whose actual values were treated as fitting parameters.) The other four could, in principal, be pinned down by three-dimensional calculations of microstructure response. We suspect that there will still be a need to have several scaling factors, however.

The surface topology function used in our erosive burning law has no experimental or theoretical support. Examination of the microstructure behavior under shock loading led us to construct a model based upon two hotspot ignition mechanisms that served to trigger erosive burning, and a competition between erosive burning and bulk reaction. The competition was one-sided, with erosive burning being much more important in all regions except those near the detonation state.

In its current state, the model should not be useful in describing the behavior of ramp waves. We believe that could be corrected by including the time evolution of hotspot formation, and the dependence of heating upon the evolving ramp wave pressure field. This can be calculated using the hydrocodes, and introduced as a model refinement. We expect that the current model will be useful in describing planar short shock behavior. Henson's work indicates that the rate determining steps occur within the solid phases, and the exothermic gas phase reaction is very fast by comparison. We expect that the short shock behavior will be best described by a competition between the growth of the shock due to reaction and the decay of the shock due to rarefactions. We also expect that the quenching of reaction will be a secondary effect. Whether or not such a model will be able to handle divergent flows, as might result from a detonator or booster remains to be seen. It should depend strongly upon the influence of the diverging flow upon the heating mechanisms. These ideas can be explored with the aid of the hydrocode microstructure descriptions, and we look forward to doing so.

ACKNOWLEDGEMENTS

We are grateful to James N. Johnson for his considerable help with his method of characteristics code, CHARADE, and to Larry Luck and David Zerkle for providing their Mathematica based method of characteristics code. We especially appreciate having access to the extraordinary gauge data generated by R. Gustavsen and colleagues. These data are superb, and will provide an excellent guide for continued model development.

REFERENCES

1. Symposium (International) on Detonation, vols 1-11, Office of Naval Research.
2. Kim, K., Sohn, C, "Modeling of Reaction Buildup Processes in Shocked Porous Explosives", *Eighth Symposium (International) on Detonation*, 926, NSWC MP 96-194, (1986).

3. Partom, Y., “Characteristics Code for Shock Initiation”. LANL Report LA 20773 + Addendum. (1986).
4. Skidmore, C., et al, “The Evolution of Microstructural Changes in Pressed HMX Explosives”, *Eleventh Symposium (International) on Detonation*, Snowmass, CO, Office of Naval Research, 556- 563, (1998).
5. Benson, D.J., “Computational Methods in Lagrangian and Eulerian Hydrocodes”, *Computer Methods in Applied Mechanics and Engineering*, 99:235-394, (1992).
6. Conley, P., “Microstructural Effects in Shock Initiation”, *Eleventh Symposium (International) on Detonation*, Snowmass, CO, Office of Naval Research, 768-780, (1998).
7. Davis, W. C., “Complete Equation of State for Unreacted Solid Explosive”, Combustion and Flame, 120:399-403 (2000).
8. Gustavsen, R. private communication.
9. Sheffield, S., et al, “Progress in Measuring Detonation Wave Profiles in PBX 9501”, *Eleventh Symposium (International) on Detonation*, Snowmass, CO, Office of Naval Research, 821-827, (1998).
10. Henson, B., private communication